Proceedings of the ASME 2008 International Design Engineering Technical Conferences & Computers and Information in Engineering Conference
IDETC/CIE 2008
August 3-6, 2008, Brooklyn, New York, USA

DETC2008-49902

DRAFT: KINEMATIC ANALYSIS OF A COMPLIANT MICROPLATFORM

Julio Correa
Department of Mechanical Engineering
Universidad Pontificia Bolivariana, Medellín, 56006, Colombia

Carl Crane
Department of Mechanical Engineering
University of Florida, Gainesville, Florida 32611, U.S.A.

Huikai Xie
Department of Electrical and Computer Engineering
University of Florida, Gainesville, Florida 32611, U.S.A.

ABSTRACT

Mechanisms formed by rigid elements are not suitable for applications at the microlevel due to manufacturing limitations. For the same reason, devices for microelectromechanical systems (MEMS) are basically planar mechanisms. This paper addresses a microplatform able to move in the three dimensional space. It is formed by bimorph actuators connected to the central platform by compliant elements. The forward and reverse analyses for the microplatform are presented.

1 INTRODUCTION

Mechanisms formed by rigid links and rigid joints have been the object of extensive studies for the theory of mechanisms. These kind of devices are well suited to work at the macro-world, however when the dimensions of the systems are on the order of microns, limitations due to manufacturing processes impose severe limitations, and the generation of motion requires alternative approaches.

Devices for microelectromechanical systems (MEMS) are basically planar devices. This is due the current manufacturing techniques that are derived from the integrated circuit industry. Creating 3D structures at the micro level is a difficult task. Most of the motion of MEMS devices is constrained to the plane. Some works have been made to create spatial motion.

Out-of-plane actuators can convert input signals into displacements normal to the surface of a substrate. Three-dimensional microdevices are useful for different tasks as for example, object positioning, micromanipulators, optical scanners, tomographic imaging, optical switches, microrelays, adjustable lenses and bio-MEMS applications.

To obtain out-of-plane motion is a challenging problem and several approaches have been proposed. Usually out-of-plane actuators are multilayer structures, although single layer devices have been reported by Chen [1]. Generally speaking current solutions are based on vertical comb drives, on the deformation of the materials or on the assembly of basic linkages.

Vertical comb drives are formed by an array of capacitors. When a voltage is applied, the movable components of the capacitors rise out of the plane. They are combined with torsion mirrors to tilt micromirrors as it is described by Milanovic [2] and Lee [3]. The vertical motion of comb drives is limited and they require a careful design and control to avoid jumps associated with the pull-in voltage, see Bronson and Wiens [4].

Combination of TiNi and Si cantilever or other substrates such as SU-8 or polymide have been used to create out-of-plane motion devices. Fu [5] reports several devices based on a TiNi film which is actuated when a current is applied to the electrode.

A micromirror having a large vertical displacement has been presented by Jain and Xie [6]. The mirror plate is attached to a rigid silicon frame by a set of aluminum/silicon dioxide bimorph beams. A polysilicon resistor is embedded within the silicon dioxide layer to form the heater for thermal bimorph actuation.

Ebefors [7] and Suh [8] implemented conveyors systems for out-of-plane motion able to perform complex manipulations. They are based on arrays of structures that can deflect out of the plane due to different coefficients of thermal expansion. Objects that are placed on the array can be moved according to the deflection of each actuator.

Schwizer [9] reports on a monolithic silicon integrated optical micro-scanner. The device consists of a mirror located on the tip of a thermal bimorph actuator beam and it is able to achieve large scan angles.

The other alternative to achieve out-of-plane motion is the assembly of planar linkages. A platform described by Jensen [10] has three degrees of freedom and the top platform remains horizontal throughout the device's motion. A proposal for a three degree of freedom parallel robot is presented by Bamberger [11]. The device uses only rigid revolute joints. Both revolute actuators are located at the base

during the manufacturing process, making the device suitable for MEMS fabrication.

Out-of-plane motion has also been realized through the use of elastic elements. A device actuated by comb drives is presented by Tung [12]. Drives are connected to a platform made of polydimethilsiloxane (PDMS) via thin flexural microjoints.

Previous works suggest that compliant links and elastic joints may be a feasible alternative to create mechanical devices at the microlevel. Figure 1 shows a schematic drawing of the device that was addressed in this research. It is radically different from the previous designs and its motion has not been studied before. The system maintains its shape due to the upward deflections of the beams. It was formed by three sets of bimorph actuators which transmitted their motion to the central platform through compliant joints. The moving platform can be described by an equilateral triangle. The fixed ends of the actuators are distributed along the vertexes of a second equilateral triangle.

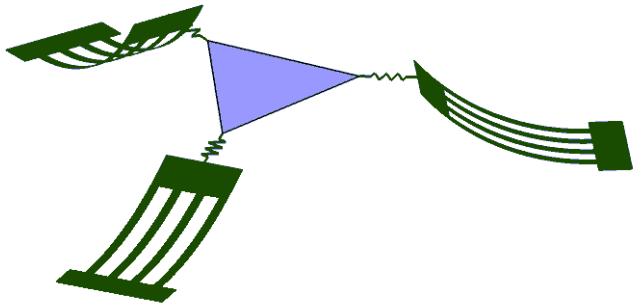

Figure 1. Schematic of the device.

The position of the device is influenced by the stiffness and free lengths of the ties, the location and nature of the joints, and the length and the current curvature of the beams. The presence of elastic elements increases the complexity of the mathematical model that describes the relations between internal forces and the positions of the beams. This paper addresses the kinematic models that describe the forward and reverse analysis of the mechanism displayed in Figure 1. The details concerning to the design and manufacturing of the device are presented in a separate work.

2 FORWARD ANALYSIS

Figure 2 depicts the device in a general position. In the forward analysis the location of points Q_i with respect to a global reference system are given and the objective is to evaluate the coordinates of points P_i with respect to the global system A. To simplify the problem, the moving platform is considered massless and the stiffness of the compliant elements are linear and equal for all three springs. Further the deflections of the actuators due to the spring forces are minimal and therefore they do not affect the kinematics of the platform.

The solution can be obtained using a Newtonian approach or an energy approach. The Newtonian approach is preferred here because it gives a better understanding of the geometry of the system.

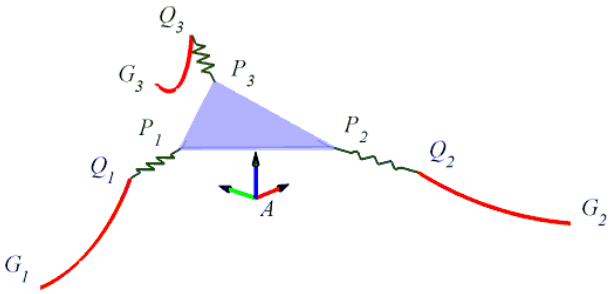

Figure 2. Device in a general position.

Since the platform is massless, the external forces acting on the platform are due only to the three springs, then equilibrium of forces yields

$$f_1\underline{s}_1 + f_2\underline{s}_2 + f_3\underline{s}_3 = \underline{0} \qquad (1)$$

where

$\underline{s}_i$: unit vector from P_i to Q_i

f_i : is the magnitude of the force in each spring.

Since the springs are linear, each force magnitude in Equation 1 can be expressed as a function of its stiffness and its deformation as

$$k(d_1 - d_0)\underline{s}_1 + k(d_2 - d_0)\underline{s}_2 + k(d_3 - d_0)\underline{s}_3 = \underline{0} \qquad (2)$$

where

d_i : actual length of the springs

d_0 : free length of the springs

When the platform is deployed from the plane, the current lengths are always greater than the free lengths, and the force magnitude coefficients in Equation 2 are different from zero. It is also apparent that vectors $\underline{s}_1$, $\underline{s}_2$, and $\underline{s}_3$ are linearly dependent. From Linear Algebra, Brand [13], a necessary and sufficient condition that three vectors be linearly dependent is that they be coplanar. From the definition of $\underline{s}_i$, this result implies that despite the spatial motion of the platform, points Q_1, Q_2, Q_3, P_1, P_2, and P_3 belong to the same plane and Equation 1 can be presented as

$$f_1\begin{bmatrix} s_{1x} \\ s_{1y} \end{bmatrix} + f_2\begin{bmatrix} s_{2x} \\ s_{2y} \end{bmatrix} + f_3\begin{bmatrix} s_{3x} \\ s_{3y} \end{bmatrix} = \underline{0} \qquad (3)$$

where

$\underline{s}_{ix}, \underline{s}_{ix}$: rectangular components of the unit vectors $\underline{s}_i$ expressed in terms of a coordinate system whose z axis is normal to the plane of the moving platform.

The moment of the force $f\underline{s}$ with respect to an arbitrary point V is a vector perpendicular to the plane of the forces with magnitude $f \cdot p$, where p is the perpendicular distance between V and the line of action of force $f\underline{s}$. The condition of equilibrium of forces requires that the summation of moments with respect to the arbitrary point V must be zero. Thus for the forces acting on the moving platform

$$f_1 p_1 + f_2 p_2 + f_3 p_3 = 0 \qquad (4)$$

Equation 3 can be combined with Equation 4 (see Duffy [14]) to obtain,

$$\begin{bmatrix} s_{1x} & s_{2x} & s_{3x} \\ s_{1y} & s_{2y} & s_{3y} \\ p_1 & p_2 & p_3 \end{bmatrix} \begin{bmatrix} f_1 \\ f_2 \\ f_3 \end{bmatrix} = \underline{0} \qquad (5)$$

Nontrivial solutions for f_i requires that

$$\begin{vmatrix} s_{1x} & s_{2x} & s_{3x} \\ s_{1y} & s_{2y} & s_{3y} \\ p_1 & p_2 & p_3 \end{vmatrix} = 0 \qquad (6)$$

This situation occurs when the forces are concurrent or parallel. For the configuration of the current device it is not possible for the forces to be parallel and therefore they must meet in a point. This fact is essential for the following derivations.

There are several ways to solve the forward analysis problem. Figure 3 depicts the variables and parameters used for the solution that is presented here.

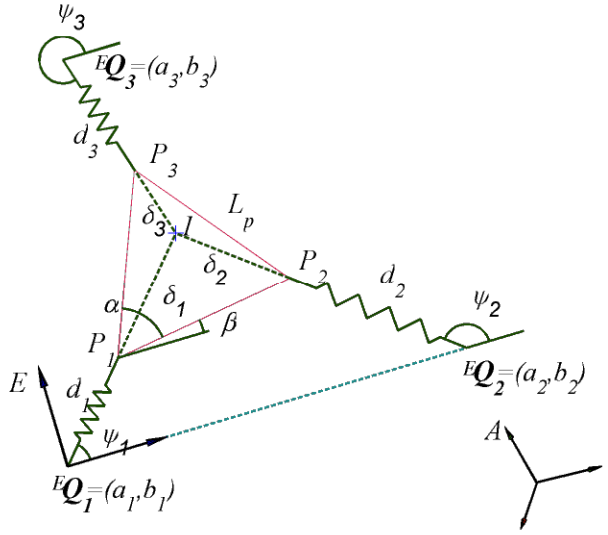

Figure 3. Nomenclature for the forward analysis.

The nomenclature defined here will be used later in the reverse analysis. The elements presented in Figure 3 are defined as follows:

- Coordinate system *A*: global reference system
- Coordinate system *E*: local reference system such that its origin is at point Q_1, the $^E\underline{x}$ axis passes through point Q_2 and the $^E\underline{z}$ axis is perpendicular to the plane of the platform
- *I*: point of intersection of the line of action of the forces acting on the platform
- P_i: point that defines the moving platform
- Q_i: free end of the actuator *i*
- a_i, b_i : coordinates of point Q_i in the local system *E*
- d_i : current length of the spring *i*
- δ_i : distance between point P_i and the intersection point *I*
- ψ_i : angle between d_i and the local x-axis
- β : angle of rotation of the platform with respect to the local x-axis
- L_p : length of a side of the equilateral platform
- α : internal angle of the moving platform and therefore equal to $\pi/3$

The global system *A* may be located in any arbitrary position. The coordinates of points Q_1, Q_2, and Q_3 are given in this system. With the knowledge of points Q_i, the local system *E* is defined as follows

$$^A\underline{x}_E = \frac{^A\underline{Q}_2 - {}^A\underline{Q}_1}{\left|{}^A\underline{Q}_2 - {}^A\underline{Q}_1\right|} \qquad (7)$$

$$^A\underline{z}_E = \frac{\left({}^A\underline{Q}_2 - {}^A\underline{Q}_1\right)\times\left({}^A\underline{Q}_3 - {}^A\underline{Q}_1\right)}{\left|\left({}^A\underline{Q}_2 - {}^A\underline{Q}_1\right)\times\left({}^A\underline{Q}_3 - {}^A\underline{Q}_1\right)\right|} \qquad (8)$$

$$^A\underline{y}_E = {}^A\underline{z}_E \times {}^A\underline{x}_E \ . \qquad (9)$$

The transformation that relates systems *A* and *E* is given by Crane [15] as

$$^A_E T = \begin{bmatrix} & ^A_E R & & ^A\underline{Q}_1 \\ 0 & 0 & 0 & 1 \end{bmatrix} \qquad (10)$$

where

$$^A_E R = \begin{bmatrix} ^A\underline{x}_E & ^A\underline{y}_E & ^A\underline{z}_E \end{bmatrix} \qquad (11)$$

The homogeneous coordinates of points Q_i in the *E* coordinate system are given by $[a_i, b_i, 0, 1]^T$ and they can be found from the relation

$$^E\underline{Q}_i = {}^E_A T \ {}^A\underline{Q}_i$$

where $^E_A T = \left({}^A_E T\right)^{-1}$

Note that $^EQ_1$ is the origin of system *E* and since Q_2 is located on the $^E\underline{x}$ axis then

$$a_1 = 0, \ b_1 = 0 \, , \ b_2 = 0 \qquad (12)$$

The device shown in Figure 3 is defined by ten unknowns that are listed in (13). The equations that will be used to solve for these parameters at equilibrium are obtained from the equilibrium of forces and kinematics considerations.

$$\begin{matrix} d_1, & d_2, & d_3 \\ \delta_1, & \delta_2, & \delta_3 \\ \psi_1, & \psi_2, & \psi_3 \\ \beta & & \end{matrix} \qquad (13)$$

From Equation 2 and the nomenclature shown in Figure 3, the equilibrium of forces evaluated in system *E* yields

$$\left(d_1 - d_0\right)\begin{bmatrix}\cos\psi_1 \\ \sin\psi_1\end{bmatrix} + \left(d_2 - d_0\right)\begin{bmatrix}\cos\psi_2 \\ \sin\psi_2\end{bmatrix} + \left(d_3 - d_0\right)\begin{bmatrix}\cos\psi_3 \\ \sin\psi_3\end{bmatrix} = \underline{0} \qquad (14)$$

Since the forces are concurrent, i.e. the lines of actions of the forces intersect, the equilibrium of moments does not give any new information. Further equations must be developed based

on the kinematics of the device expressed in the system E. From Figure 3 it is clear that

$$\delta_1 \ e^{i\psi_1} = L_p \ e^{i\beta} + \delta_2 \ e^{i\psi_2} \quad (15)$$

$$\delta_1 \ e^{i\psi_1} = L_p \ e^{i(\beta+\alpha)} + \delta_3 \ e^{i\psi_3} \quad (16)$$

Loops defined by $Q_1 - Q_2 - I$ and $Q_1 - Q_3 - I$ yield

$$(d_1+\delta_1) \ e^{i\psi_1} = {}^E\underline{Q}_2 - {}^E\underline{Q}_1 + (d_2+\delta_2) \ e^{i\psi_2}$$

$$(d_1+\delta_1) \ e^{i\psi_1} = {}^E\underline{Q}_3 - {}^E\underline{Q}_1 + (d_3+\delta_3) \ e^{i\psi_3}$$

Considering Equation 12, the last two equations can be simplified to

$$(d_1+\delta_1) \ e^{i\psi_1} = \begin{bmatrix} a_2 \\ 0 \end{bmatrix} + (d_2+\delta_2) \ e^{i\psi_2} \quad (17)$$

$$(d_1+\delta_1) \ e^{i\psi_1} = \begin{bmatrix} a_3 \\ b_3 \end{bmatrix} + (d_3+\delta_3) \ e^{i\psi_3} \quad (18)$$

The scalar components of Equations 14 through 18 form a nonlinear system that can be solved using numerical methods. A program to solve the mathematical model for the forward analysis was implemented. The program takes advantage of a function that implements the Newton-Raphson method. Once the variables are found, the points ${}^A\underline{P}_i$ are evaluated using the transformation

$${}^A\underline{P}_i = {}^A_E T \ {}^E\underline{P}_i \quad (19)$$

where the points ${}^E\underline{P}_i$ are given by (see Figure 3)

$${}^E\underline{P}_1 = {}^E\underline{Q}_1 + d_1 \begin{bmatrix} \cos\psi_1 \\ \sin\psi_1 \end{bmatrix} \quad (20)$$

$${}^E\underline{P}_2 = {}^E\underline{P}_1 + L_p \begin{bmatrix} \cos\beta \\ \sin\beta \end{bmatrix} \quad (21)$$

$${}^E\underline{P}_3 = {}^E\underline{P}_1 + L_p \begin{bmatrix} \cos(\beta+\alpha) \\ \sin(\beta+\alpha) \end{bmatrix} \quad (22)$$

One way to verify the validity of the results is to check if they satisfy the equilibrium equations and if the lines of action of the forces intersect at the same point when they are evaluated in the global system A instead of the local system E. The equilibrium condition in the global system can be written as

$$\Sigma\underline{F} = k(d_1 - d_0)\underline{s}_1 + k(d_2 - d_0)\underline{s}_2 + k(d_3 - d_0)\underline{s}_3 \quad (23)$$

where

$$\underline{s}_i = \frac{{}^A\underline{Q}_i - {}^A\underline{P}_i}{\left| {}^A\underline{Q}_i - {}^A\underline{P}_i \right|}$$

The intersection point of the lines passing through points $P_1 - Q_1$ and $P_2 - Q_2$ is given by (Crane, C., Rico, J., Duffy, J., Screw Theory for Spatial Robot Manipulators, Cambridge University Press, in Preparation) as

$${}^A\underline{r}_{12} = \frac{\underline{s}_2 \times \underline{s}_{02} - (\underline{s}_1 \cdot \underline{s}_2)\underline{s}_1 \times \underline{s}_{02} + (\underline{s}_1 \times \underline{s}_{01} \cdot \underline{s}_2)\underline{s}_2}{1 - (\underline{s}_1 \cdot \underline{s}_2)^2} \ . \quad (24)$$

Similarly, the intersection of lines passing through $P_2 - Q_2$ and $P_3 - Q_3$ is given by

$${}^A\underline{r}_{23} = \frac{\underline{s}_3 \times \underline{s}_{03} - (\underline{s}_2 \cdot \underline{s}_3)\underline{s}_2 \times \underline{s}_{03} + (\underline{s}_2 \times \underline{s}_{02} \cdot \underline{s}_3)\underline{s}_3}{1 - (\underline{s}_2 \cdot \underline{s}_3)^2} \quad (25)$$

where

$$\underline{s}_{0i} = {}^A\underline{Q}_i \times \underline{s}_i$$

Lines of action of the external forces intersect if ${}^A\underline{r}_{12} = {}^A\underline{r}_{23}$.

3 REVERSE ANALYSIS

In the reverse analysis the objective is to find the location of the actuators in order to obtain a desired output. Since there are no external forces or moments applied to the platform, it is not possible to achieve an arbitrary location and orientation. However it is feasible to constrain the moving platform to be perpendicular to a given vector $\underline{n}$ (Figure 4).

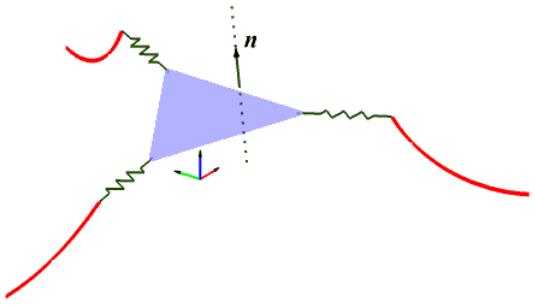

Figure 4. Normal vector to the moving platform.

The motion of the free end of the actuator is the caused by the bending of the bimorph beam due to an increase of temperature. The bending is a function of the thermal resistance and the applied voltage. Figure 5a shows the path of the free end for several positions of the beam. Lowell [16] has shown that for the purpose of analysis, compliant elements can be replaced by hypothetical rigid binary links. Figure 5b shows how the original path of the free end can be approximated for a link whose center lies on the horizontal axis and with a radius t forming an angle θ with the horizontal. The path of the free end may be obtained experimentally and the center and radius of the hypothetical link adjusted by fitting the curve.

Since all the beams are equal, the radius t is equal for all the actuators and the location of E with respect to G is also the same for all the actuators. In the following developments it will be assumed that points E_i and radius t are already evaluated.

The reverse problem for this device admits different formulations, considering which parameters are considered as given and which must be evaluated. The current research presents two cases.

3.1 Reverse Analysis Case 1:

This case may be stated as follows: given the position of the free end of one of the actuators and a unit vector perpendicular to the moving platform, find the position of the free ends of the remaining actuators.

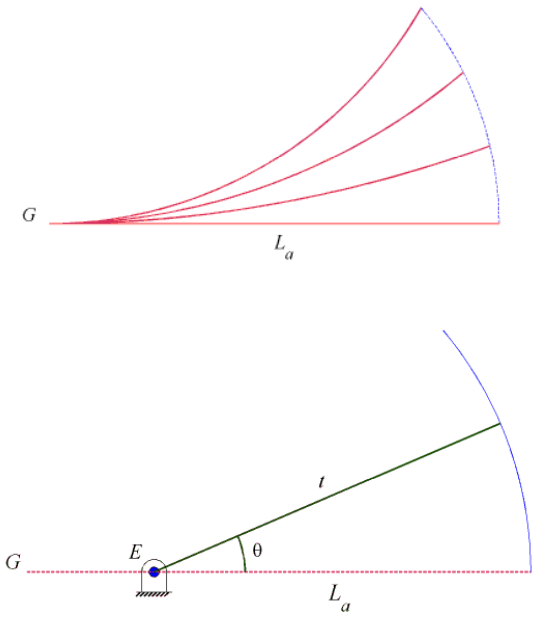

Figure 5. Path of the free end. a) Original path. b) Approximated path.

Figure 6 shows the plane that contains the moving platform and the actuators represented as binary links. The unit vector $\underline{n}$ is perpendicular to this plane and the positions of points Q_i can be defined by the vectors $\underline{r}_i$ in a global reference system.

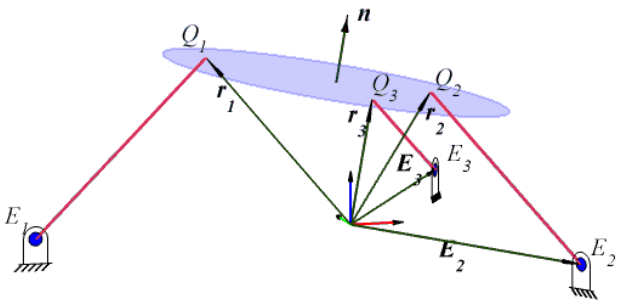

Figure 6. Parameters for the reverse analysis, case 1.

One sequence of transformations that relates the global system and any of the local systems located at the fixed pivots of the binary links and whose x-axes are aligned with the axes of the binary links (Figure 6), is

$$ {}^{A}_{L}T = Translation(E_i) * Rotation(z,\gamma_i) * Rotation(y,\theta_i) \quad (26) $$

$$ {}^{A}_{L}T = \begin{bmatrix} \cos\gamma_i \cos\theta_i & -\sin\gamma_i & \cos\gamma_i \sin\theta_i & E_{ix} \\ \sin\gamma_i \cos\theta_i & \cos\gamma_i & \sin\gamma_i \sin\theta_i & E_{iy} \\ -\sin\theta_i & 0 & \cos\theta_i & 0 \\ 0 & 0 & 0 & 1 \end{bmatrix} \quad (27) $$

When $i=1, 2, 3$ references systems B, C and D are obtained. Figure 7a shows a top view when only the first two transformations of Equation 26 are carried out. Note that angles γ_i are constant. Figure 7b illustrates the local reference systems in their final orientation after performing the last transformation involving θ_i in Equation 26.

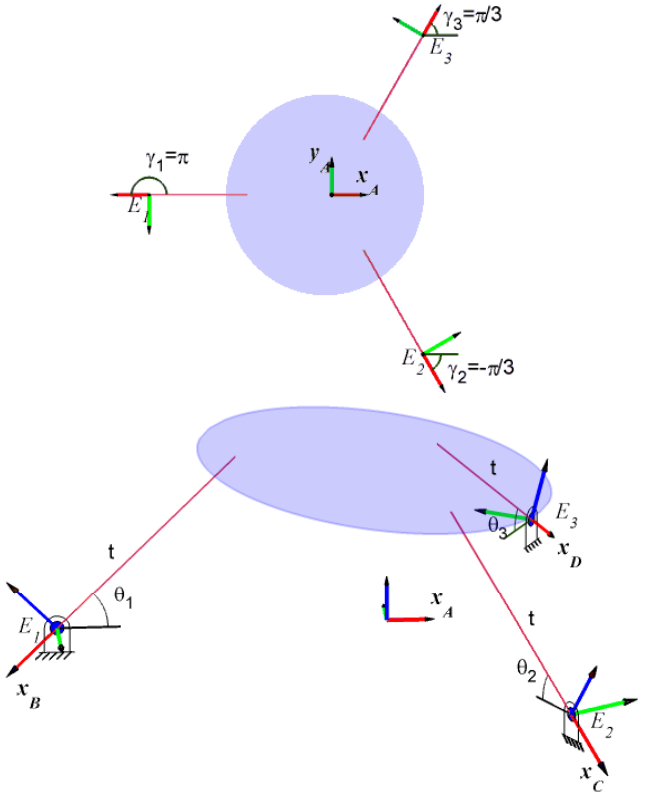

Figure 7. Location of the local reference systems for the reverse analysis. a) First rotation. b) Second rotation.

The first three elements of the first column of Equation 27 represent the local x-axis expressed in the global system A. In particular the local axis ${}^{A}\underline{x}_C$ is obtained by substituting $i=2$ in Equation 27 to give

$$ {}^{A}\underline{x}_C = \begin{bmatrix} \cos\gamma_2 \cos\theta_2 \\ \sin\gamma_2 \cos\theta_2 \\ -\sin\theta_2 \end{bmatrix} . \quad (28) $$

Without lost of generality assume that ${}^{A}\underline{Q}_1$ is the free end whose position is given. Then the vector $\underline{r}_1$ is known. From the equation of a plane (Crane, C., Rico, J., Duffy, J., Screw Theory for Spatial Robot Manipulators, Cambridge University Press, in Preparation), and Figure 6

$$ (\underline{r}_2 - \underline{r}_1)\cdot \underline{n} = 0 \quad \therefore \quad \underline{r}_2 \cdot \underline{n} = \underline{r}_1 \cdot \underline{n} \quad (29) $$

From the geometry of the device (Figure 6)

$$ \underline{r}_2 = \underline{E}_2 + \underline{t}_2 \quad (30) $$

where t_2 is the vector from point E_2 to point Q_2.

From Figure 7 and considering Equation 28

$$ \underline{t}_2 = -t\ {}^{A}\underline{x}_C = -t \begin{bmatrix} \cos\gamma_2 \cos\theta_2 \\ \sin\gamma_2 \cos\theta_2 \\ -\sin\theta_2 \end{bmatrix} . \quad (31) $$

The scalar product of Equation 30 with $\underline{n}$ yields

$$ \underline{r}_2 \cdot \underline{n} = \underline{E}_2 \cdot \underline{n} + \underline{t}_2 \cdot \underline{n} \quad (32) $$

Substituting Equations 29 and 31 into Equation 32 yields

$$\underline{r}_1 \cdot \underline{n} = \underline{E}_2 \cdot \underline{n} - t\begin{bmatrix} n_x & n_y & n_z \end{bmatrix}\begin{bmatrix} \cos\gamma_2 \cos\theta_2 \\ \sin\gamma_2 \cos\theta_2 \\ -\sin\theta_2 \end{bmatrix} \quad (33)$$

Regrouping Equation 33 yields

$$A_2 \cos\theta_2 + B_2 \sin\theta_2 + D_2 = 0 \quad (34)$$

where

$$A_2 = n_x \cos\gamma_2 + n_y \sin\gamma_2 \quad (35)$$

$$B_2 = -n_z \quad (36)$$

$$D_2 = \frac{\underline{r}_1 \cdot \underline{n} - \underline{E}_2 \cdot \underline{n}}{t} \quad (37)$$

It is possible to obtain a closed solution for θ_2 in Equation 34, (see Crane [15]). Substituting the value of θ_2 in Equation 31 and the result in Equation 30, the coordinates of $\underline{r}_2$, and therefore of point ${}^A\underline{Q}_2$, are determined.

The evaluation of values for θ_3 follows a similar procedure. From Figure 6

$$\underline{r}_3 \cdot \underline{n} = \underline{r}_1 \cdot \underline{n} \quad (38)$$

where,

$$\underline{r}_3 = \underline{E}_3 + t\,{}^A\underline{x}_D \quad (39)$$

The vector ${}^A\underline{x}_D$ is given by the first three rows of the third column in Equation 27 when $i=3$. Substituting the expression for ${}^A\underline{x}_D$ into Equation 39 and the result into Equation 38 and rearranging terms, the angle $\theta_3$is given by

$$A_3 \cos\theta_3 + B_3 \sin\theta_3 + D_3 = 0 \quad (40)$$

where

$$A_3 = n_x \cos\gamma_3 + n_y \sin\gamma_3 \quad (41)$$

$$B_3 = -n_z \quad (42)$$

$$D_3 = \frac{\underline{r}_1 \cdot \underline{n} - \underline{E}_3 \cdot \underline{n}}{t} \quad (43)$$

Equation 40 permits one to evaluate θ_3 and then Equation 39 yields $\underline{r}_3$ and therefore ${}^A\underline{Q}_3$. The reverse analysis for this case is completed.

3.2 Reverse Analysis Case 2:

For the second case, one could desire to include information about the location of points in the moving platform in the reverse analysis. Since there are no external forces acting on the mechanism, it is not possible to specify a general position for one point of the platform. However it is feasible to specify, in addition to the orientation of the platform given by the vector perpendicular to its plane, the height with respect to the horizontal plane of one of the points of the platform. Any point is equally appropriate, for this case the point ${}^A\underline{P}_1$ is selected (Figure 8).

In case 1 it was possible to obtain a closed solution easily because it did not involve any information regarding the location of the points on the moving platform. In the new situation, the mathematics are more involved and requires a numerical technique for its solution.

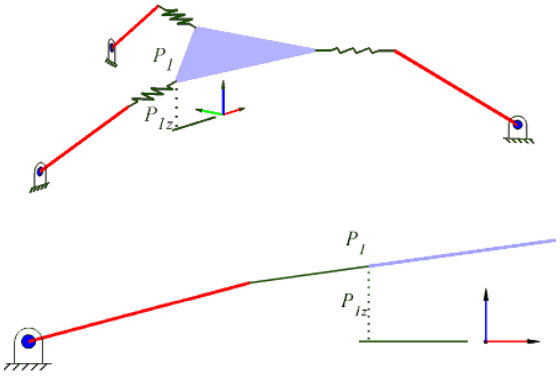

Figure 8. Prescribed vertical component of point P1. a) Isometric view. b) Lateral view.

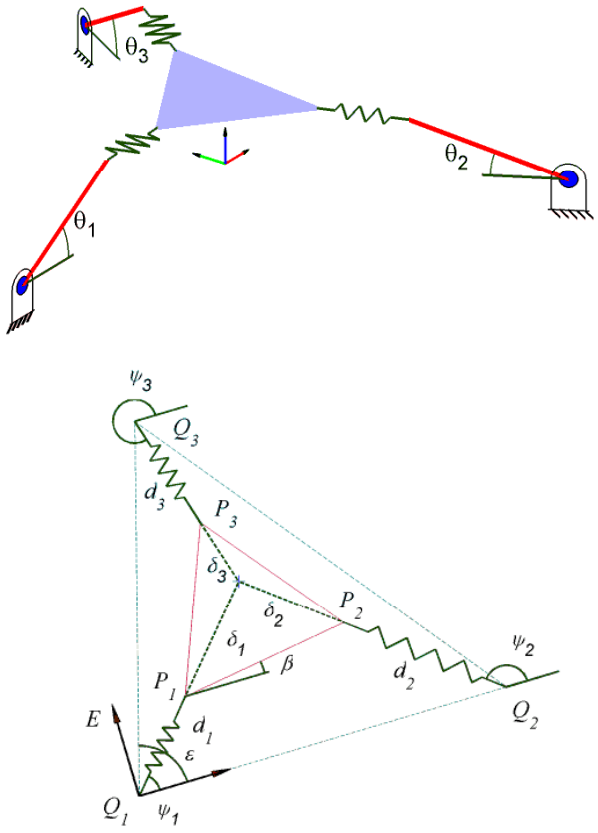

Figure 9. Nomenclature for the reverse analysis, case 2. a) Isometric view. b) Plane of the forces.

Figure 9a shows the device in an arbitrary position. Figure 9b shows the variables located on the plane of the moving platform. Positions of points ${}^A\underline{Q}_i$ are unknown and depend on angles θ_i. Angle ε is also an unknown as well as the x and y coordinates of point ${}^A\underline{P}_1$ (coordinates of ${}^A\underline{P}_2$ and ${}^A\underline{P}_3$ can be found once the model is solved). Therefore, in addition to the ten variables used in the forward analysis and enumerated in (13), here there are six new unknowns: θ_1, θ_2, θ_3, ε, P_{1x}, and P_{1y}. The solution requires 16 equations.

The reverse analysis for this case may be posed as follows: given the unit vector $\underline{n}$ perpendicular to the moving platform and the scalar component z of the vector ${}^{A}\underline{P}_1$, find the location of the free ends of the binary links ${}^{A}\underline{Q}_i$, the scalar components x and y of the vector ${}^{A}\underline{P}_i$ and the location of the remaining vertexes of the moving platform ${}^{A}\underline{P}_2$ and ${}^{A}\underline{P}_3$.

Equation 27 can be used to relate points $\underline{Q}_i$ expressed in the local systems at the fixed pivots (Figure 7) to system A as

$$ {}^{A}\underline{Q}_i = {}^{A}_{L}T\,{}^{L}\underline{Q}_i \qquad (44) $$

where

$$ {}^{L}Q_i = \begin{bmatrix} -t & 0 & 0 & 1 \end{bmatrix}^T \qquad (45) $$

Substituting Equations 27 and 45 into Equation 44 yields

$$ {}^{A}\underline{Q}_i = \begin{bmatrix} -t\cos\gamma_i\cos\theta_i + E_{ix} \\ -t\sin\gamma_i\cos\theta_i + E_{iy} \\ t\sin\theta_i \\ 1 \end{bmatrix}, \; i = 1,2,3\,. \qquad (46) $$

With Equation 46 it is possible to express distances $\overline{Q_iQ_j}$ between points ${}^{A}\underline{Q}_i$ and ${}^{A}\underline{Q}_j$ in terms of θ_i as

$$ \overline{Q_1Q_2} = \left| {}^{A}\underline{Q}_2 - {}^{A}\underline{Q}_1 \right| \qquad (47) $$

$$ \overline{Q_2Q_3} = \left| {}^{A}\underline{Q}_3 - {}^{A}\underline{Q}_2 \right| \qquad (48) $$

$$ \overline{Q_1Q_3} = \left| {}^{A}\underline{Q}_3 - {}^{A}\underline{Q}_1 \right| \,. \qquad (49) $$

where it is understood that points ${}^{A}\underline{Q}_i$, in Equations 47 throughout 49 are expressed in Cartesian coordinates instead of homogeneous coordinates.

The relation between ${}^{E}\underline{P}_1$ and ${}^{A}\underline{P}_1$ is given by

$$ {}^{A}\underline{P}_1 = {}^{A}_{E}T\;{}^{E}\underline{P}_1\,. \qquad (50) $$

The transformation ${}^{A}_{E}T$ defines the relation between the global system A and a reference system E whose origin is located at ${}^{A}\underline{Q}_1$ with its x-axis pointing from ${}^{A}\underline{Q}_1$ to ${}^{A}\underline{Q}_2$, and for which the z-axis is the unit vector $\underline{n}$ (Figure 9). Thus this transformation may be written as

$$ {}^{A}_{E}T = \begin{bmatrix} {}^{A}\underline{x}_E & {}^{A}\underline{y}_E & {}^{A}\underline{z}_E & {}^{A}\underline{Q}_1 \\ 0 & 0 & 0 & 1 \end{bmatrix} \qquad (51) $$

where

$$ {}^{A}\underline{x}_E = \frac{{}^{A}\underline{Q}_2 - {}^{A}\underline{Q}_1}{\left| {}^{A}\underline{Q}_2 - {}^{A}\underline{Q}_1 \right|} \qquad (52) $$

$$ {}^{A}\underline{z}_E = \underline{n} \qquad (53) $$

$$ {}^{A}\underline{y}_E = {}^{A}\underline{z}_E \times {}^{A}\underline{x}_E \quad . \qquad (54) $$

The coordinates of ${}^{E}\underline{P}_1$ can be obtained from Figure 9 as $[d_1\cos\psi_1,\, d_1\sin\psi_1,\, 0]^T$ and inserting this in Equation 50 yields

$$ \begin{bmatrix} {}^{A}P_{1x} \\ {}^{A}P_{1y} \\ {}^{A}P_{1z} \\ 1 \end{bmatrix} = \begin{bmatrix} r_{11} & r_{12} & r_{13} & {}^{A}Q_{1x} \\ r_{21} & r_{22} & r_{23} & {}^{A}Q_{1y} \\ r_{31} & r_{32} & r_{33} & {}^{A}Q_{1z} \\ 0 & 0 & 0 & 1 \end{bmatrix} \begin{bmatrix} d_1\cos\psi_1 \\ d_1\sin\psi_1 \\ 0 \\ 1 \end{bmatrix} . \qquad (55) $$

where the terms r_{ij} depend only on θ_i.

At this point all the developments required for the mathematical model are obtained. Expression 55 yields three scalar equations, one of them involving the prescribed value ${}^{A}P_{1z}$, and thus

$$ {}^{A}P_{1x} = r_{11}d_1\cos\psi_1 + r_{12}d_1\sin\psi_1 + {}^{A}Q_{1x} \qquad (56) $$

$$ {}^{A}P_{1y} = r_{21}d_1\cos\psi_1 + r_{22}d_1\sin\psi_1 + {}^{A}Q_{1y} \qquad (57) $$

$$ {}^{A}P_{1z} = r_{31}d_1\cos\psi_1 + r_{32}d_1\sin\psi_1 + {}^{A}Q_{1z}\,. \qquad (58) $$

The angle ε in Figure 9 can be related to points ${}^{A}\underline{Q}_i$ using the cosine law

$$ \overline{Q_2Q_3}^2 = \overline{Q_1Q_2}^2 + \overline{Q_1Q_3}^2 - 2\overline{Q_1Q_2} * \overline{Q_1Q_3} * \cos\varepsilon \qquad (59) $$

where the terms $\overline{Q_iQ_j}$ are given by Equations 47 through 49.

Equilibrium conditions can be expressed in the plane of the moving platform as it was done in the forward analysis as

$$ (d_1 - d_0)\cos\psi_1 + (d_2 - d_0)\cos\psi_2 + (d_3 - d_0)\cos\psi_3 = 0 \qquad (60) $$

$$ (d_1 - d_0)\sin\psi_1 + (d_2 - d_0)\sin\psi_2 + (d_3 - d_0)\sin\psi_3 = 0\,. \qquad (61) $$

The geometry equations (15) and (16) that were used in the forward analysis problem are still valid here and are rewritten as (Figure 9)

$$ \delta_1 e^{i\psi_1} = L_p e^{i\beta} + \delta_2 e^{i\psi_2} \qquad (62) $$

$$ \delta_1 e^{i\psi_1} = L_p e^{i(\alpha+\beta)} + \delta_3 e^{i\psi_3}\,. \qquad (63) $$

The geometry relations for the actual lengths of the springs involve the terms $\overline{Q_1Q_2}, \overline{Q_1Q_3}$ and ε (Figure 9) and are written as

$$ (d_1 + \delta_1)e^{i\psi_1} = \overline{Q_1Q_2}e^{i0} + (d_2 + \delta_2)e^{i\psi_2} \qquad (64) $$

$$ (d_1 + \delta_1)e^{i\psi_1} = \overline{Q_1Q_3}e^{i\varepsilon} + (d_3 + \delta_3)e^{i\psi_3}\,. \qquad (65) $$

The vectors from ${}^{A}\underline{Q}_1$ to ${}^{A}\underline{Q}_2$ and from ${}^{A}\underline{Q}_1$ to ${}^{A}\underline{Q}_3$ must be perpendicular to vector $\underline{n}$. These constraints introduce the two additional relations

$$ \left({}^{A}\underline{Q}_2 - {}^{A}\underline{Q}_1\right)\cdot\underline{n} = 0 \qquad (66) $$

$$ \left({}^{A}\underline{Q}_3 - {}^{A}\underline{Q}_1\right)\cdot\underline{n} = 0\,. \qquad (67) $$

Equations 58 through 67 form a system of 14 equations and 14 unknowns that can be solved for θ_1, θ_2, θ_3, ε, d_1, d_2, d_3, δ_1, δ_2, δ_3, ψ_1, ψ_2, ψ_3, and β using numerical methods. Once the solution is obtained, it is possible to evaluate ${}^{A}\underline{Q}_i$ using Equation 46. Coordinates ${}^{A}P_{1x}$ and ${}^{A}P_{1y}$ are easily evaluated using Equations 56 and 57. In this way point ${}^{A}\underline{P}_1$ is determined.

To complete the reverse analysis for the current case it is necessary to evaluate ${}^{A}\underline{P}_2$ and ${}^{A}\underline{P}_3$. A coordinate system F is defined as parallel to system E and located at ${}^{A}\underline{P}_1$, (Figure 9), and the transformation matrix that relates coordinate systems F and A can be written as

$$ {}^{A}_{F}T = \begin{bmatrix} {}^{A}\underline{x}_E & {}^{A}\underline{y}_E & {}^{A}\underline{z}_E & {}^{A}\underline{P}_1 \\ 0 & 0 & 0 & 1 \end{bmatrix} . \qquad (68) $$

The terms corresponding to the rotation matrix are obtained from Equations 52 throughout 54 and with the aid of Figure 9 the following relations are obtained, which complete the second case for the reverse analysis.

$$ {}^{A}\underline{P}_2 = {}^{A}_{F}T \; {}^{F}\underline{P}_2 \quad , \qquad {}^{F}\underline{P}_2 = \begin{bmatrix} L_p \cos\beta \\ L_p \sin\beta \\ 0 \\ 1 \end{bmatrix} \tag{69} $$

$$ {}^{A}\underline{P}_3 = {}^{A}_{F}T \; {}^{F}\underline{P}_3 \quad , \qquad {}^{F}\underline{P}_3 = \begin{bmatrix} L_p \cos(\beta+\alpha) \\ L_p \sin(\beta+\alpha) \\ 0 \\ 1 \end{bmatrix} \tag{70} $$

4 CONCLUSIONS

In this research a new micro-scaled platform was introduced that can be fabricated in the plane and yet is able to perform three dimensional motions. The primary contribution of the paper is the analysis of this mechanism, specifically the derivation of the forward and reverse kinematic analyses which are required for basic control of the device.

Several practical applications for the device are anticipated. For example the moving platform could be a mirror whose orientation and height above the base can be controlled. A second application is related to micro-assembly where the compliance in the device inherently limits contact forces. In this application a series of 'finger tips', albeit with small workspace, can be used to position and orient components for assembly.

Future work will focus on prototype fabrication and testing. Of particular interest are the impact of thermal issues on controllability and the analysis of the system dynamic behavior which is essential to the understanding of overall vibration and control issues.

5 REFERENCES

[1] Chen,W., Chien, C. Hsieh, J. , and Fang, W., 2003, "A Reliable Single-Layer Out-of-Plane Micromachined Thermal Actuator," Sensors and Actuators A, **103**(1-2), pp. 48-58.

[2] Milanovic, V., 2004, "Multilevel Beam SOI-MEMS Fabrication and Applications," Journal of Microelectromechanical Systems, **13**(1), pp 19-30.

[3] Lee,C., 2004, "Design and Fabrication of Epitaxial Silicon Micromirror Devices," Sensors and Actuators A, **115**, pp 581-590.

[4] Bronson, J.R., and Wiens, G. J., 2006, "Control of Micro Mirrors for High Precision Performance," *Proceedings of the Florida Conference on Recent Advances in Robotics*, Miami, FL, May.

[5] Fu Y., Du H., Huang W., and Hu, M., 2004, "TiNi-Based Thin Films in MEMS Applications: a Review," Sensors and Actuators A, **112**(2-3), pp. 395–408.

[6] Jain, A., Qu, H., Todd, S, Xie, H., 2005, "A Thermal Bimorph Micromirror with Large Bi-directional and Vertical Actuation," Sensors and Actuators A, **122**(1), pp. 9-15.

[7] Ebefors, T., Mattsson, J., Kalvesten, E. and Stemme, G., 1999, "A Robust Micro Conveyer Realized By Arrayed Polymide Joint Actuators," *Proceedings Twelfth IEEE Conference on Micro Electro Mechanical Systems*, Orlando, FL, January, pp. 576-581.

[8] Suh, J., Darling, R., Bohringer, K., Donald, B., Baltes, H., and Kovacs, G., 1999, "CMOS Integrated Ciliary Actuator Array as a General-Purpose Micromanipulation Tool for Small Objects," Journal of Microelectromechanical Systems, **8**(4), pp. 483-496.

[9] Schweizer, S., Calmes, S., Laudon, M., and Renaud, P., 1999, "Thermally Actuated Optical Microscanner with Large Angle and Low Consumption," Sensors and Actuators A, **76**(1-3), pp. 470–477.

[10] Jensen K., Howell L., and Lusk K. 2004, "Force Relationships for an XYZ Micromanipulator with Three Translational Degrees of Freedom," *Proceedings Design Engineering Technical Conferences*, ASME, Salt Lake City, Utah, USA, September.

[11] Bamberger, H. and Shoham, M., 2004, "Kinematic Structure of a Parallel Robot for MEMS Fabrication," *Proceedings On Advances in Robot Kinematics*, Netherlands, pp. 113-122.

[12] Tung, Y., and Kurabayashi, K., 2005, "A Single-Layer PDMS-on-Silicon Hybrid Microactuator with Multi-Axis Out-Of-Plane Motion Capabilities - Part I: Design and Analysis," Journal of Microelectromechanical Systems, **14**(3), pp. 548-557.

[13] Brand, L., 1947, *Vector and Tensor Analysis*, Wiley, New York.

[14] Duffy, J., 1996, *Statics and Kinematics with Applications to Robotics*, Cambridge University Press, New York.

[15] Crane, C., and Duffy, J., 1998, *Kinematic Analysis of Robot Manipulators*, Cambridge University Press, USA.

[16] Howell, L. L., 2001, *Compliant Mechanisms*, Wiley, New York.